Journal of Materials and Environmental Science
ISSN : 2028-2508
e-ISSN : 2737-890X
CODEN : JMESCN

J. Mater. Environ. Sci., 2026, Volume 17, Issue 8, Page 1290-1306

http://www.jmaterenvironsci.com

Production, characterization and application of activated carbons derived from local biomass for the removal of emerging water contaminants: linking the circular economy to the blue economy

Romarique Ouédraogo [1], Yacouba Sanou [1*], Moussa Fofana [2], Samuel Paré [1]

[1] *Laboratory of Analytical, Environmental and Bio-Organic Chemistry, University Joseph KI-ZERBO, 03 BP7021, Ouagadougou, Burkina Faso.*

[2] *Office of Mines and Geology of Burkina Faso, Ouagadougou, Burkina Faso.*

**Corresponding author, Email address: prosperyacson@gmail.com*

Received *01 June 2026,*
Revised *31 July 2026,*
Accepted *27 Aug 2026*

Keywords:
- ✓ *Adsorption*
- ✓ *Activated carbons;*
- ✓ *Circular economy;*
- ✓ *Cyanide;*
- ✓ *Methylene blue.*

Citation*: Ouédraogo R., Sanou Y., Fofana M., Paré S. (2026) Adsorption of emerging water contaminants onto activated carbons derived from local biomass: From circular economy to blue economy, J. Mater. Environ. Sci., 17(8), 1290-1306*

Abstract: In Burkina Faso, the increasing presence of emerging contaminants such as cyanide and dyes from water resources is a major environmental concern related to sanitary diseases. To mitigate this problem, water treatment based on adsorption with local materials offers promising and sustainable alternatives instead to conventional treatment. This work investigated the adsorption potential of activated carbons to remove cyanide and methylene blue (MB)for water purification. The multi-scale methodological approach has combined the production and characterization of activated carbons, experimental applications, and chemical modeling of the retention of emerging pollutants. Activated carbons (AC) were produced by pyrolysis of rice husks at 650°C followed by chemical and physical activation. Batch experiments were carried out using synthetic solutions of cyanide and MB and operating conditions were optimized. Results of characterization of AC indicated their carbonaceous and microporous structure. The cyanide removal rate achieved 97% at pH ≥ 11 while 98.32% of MB was removed for 60 min of contact. Monolayer chemisorption was the mechanism governing the removal of the targeted contaminants, following a pseudo-second-order kinetic. Consequently, these remediation methods contribute to the prevention of health risks, the valorization of agricultural wastes and the development of innovative solutions.

1. Introduction

In developing countries, industrial activities related to mining extraction and the local production of Koko Dunda loincloths, while essential to community incomes, involve the use of chemical substances such as cyanide and dyes. The uncontrolled use of these substances and their residual wastes are source of releasing of emerging pollutants into the aquatic environment. Cyanides are highly toxic compounds that can cause adverse effects on human and animal health (Tchounwou *et al.*, 2012). Due to their toxicity and persistence in the environment, the management of cyanide residues from mining effluents became an environmental issue in developing countries. Furthermore, the increase of industrial activities from textile, pharmaceutical, and chemical compagnies is leading to the discharge of synthetic dyes in environment (Haruna *et al.*, 2020), (Akartasse *et al.*, 2022), (Sakr *et al.*, 2015). Among these dyes, methylene blue (MB) is one of particular concerns due to its environmental persistence, toxicity, and sanitary effects (Sakr *et al.*, 2015).

In this context, it is essential to find out the innovative, accessible, and sustainable technologies for the removal of emerging pollutants associated to the effective and ecological management of cyanide residues and dyes. Several conventional methods based on advanced oxidation techniques, membrane filtration, coagulation-flocculation, electrocoagulation, ion exchange, and biological processes have been developed for water purification (Botz, 2001), (Gao *et al.*, 2016), (Hou *et al.*, 2020). In the implementation, most of these methods are complex, costly effective and less efficient for water charged with high concentrations of pollutant. Thus, adsorption onto local materials appeared to be a promising and sustainable alternative to conventional methods in developing countries. It is a highly advantageous method due to its simplicity, effectiveness, and affordable implementation cost. Its implementation requires the use of adsorbent materials such as clays, laterites, ferric oxides, and clay minerals (Dash *et al.*, 2009), (Moussavi and Khosravi, 2011), (Halet *et al.*, 2015), (Sanou *et al.*, 2021). These solids are often ineffective and non-selective during the adsorption of a pollutant in a complex aqueous environment. Therefore, activated carbons are revealed technically viable adsorbents and a preferred choice because of their textural and chemical properties favorable to the adsorption of many contaminants.

Activated carbons are obtained by pyrolysis of renewable raw materials such as rice husks, peanut shells, shea shells, corn stalks, or any agricultural waste (Kumar *et al.*, 2016), (Sanou *et al.*, 2016), (Ahmad *et al.*, 2020), (Haoufazane *et al.*, 2025). This recycling of agricultural wastes appears as a promising alternative for waste valorization, contributing to the circular economy. However, their valorization in an integrated approach directed to the blue economy remains insufficiently explored because the most of commercial carbons in the world are used in mining extraction. The use of activated carbons for water treatment as water depollution technique contributes to the blue economy. Previous studies showed that activated carbons derived from rice husks can exhibit competitive adsorption capacities for various pollutants (Mohan *et al.*, 2014), (Bhatnagar and Sillanpää, 2011), (Tchuifon *et al.*, 2016). In the frame of our contribution based on circular economy for the achievement of blue economy, activated carbons were produced from the pyrolysis of agricultural wastes. In addition, these carbons were used for the wastewater treatment by removing methylene blue and cyanide.

This study aimed to evaluate the adsorption capacity of two activated carbons for the treatment of contaminated wastewaters. More specifically, it involved the production and characterization of activated carbons from rice husks, and the evaluation of its efficiency in the removal of cyanide and methylene blue under various conditions.

2. Methodology

2.1 Preparation of activated carbons

2.1 Sampling of rice husks

Rice husks (paddy variety) were collected from the rice production site of Gampela village (12.41°N, -1.39°W), located on the eastern outskirts of Ouagadougou (**Figure 1**). To ensure representative samples, several sampling points were selected by taking care to avoid any external contamination. The collected samples were carefully packaged and labeled with essential data regarding their origin and collection conditions.

2.1.2. Production of activated carbons

Activated carbons were produced according to the method described by Chen *et al.* (2012). Indeed, raw rice husks (RRH) were washed with tap and distilled water, and then dried at 60°C for

72 h in an oven. For chemical activation, 250 mL of 1 M HCl were added to 25 g of pretreated rice husks (PRH) in an Erlenmeyer flask, with an impregnation ratio PRH/HCl (w/w) of 2.66 and the mixture was heated at 62°C for 3 h. After cooling, the mixture was filtered and the leached rice husks (LRH) were collected to be washed at pH close to 7 before the drying in the oven. Subsequently, 100 g of LRH was pyrolyzed in a mold furnace (HERAEUS) at 650°C with a rise speed of 10°C/min for 2 h under a nitrogen flow rate of 0.1 m³/h. The resulting activated carbon was named CA1. For physical activation, 100 g of PRH were pyrolyzed under an inert atmosphere (P = 1.5 bar) to obtain the carbon named CA2.

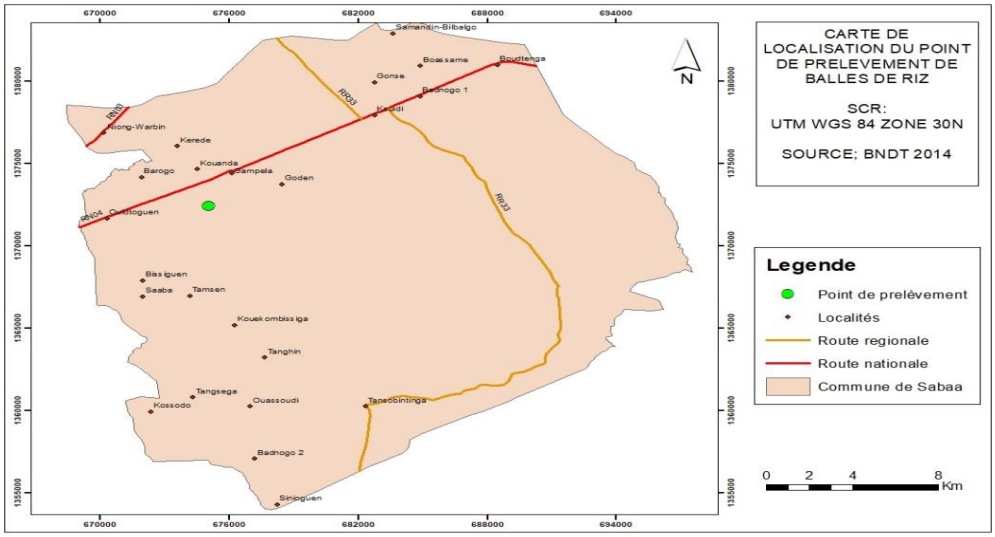

Figure 1. Localization map of sampling point of rice husks

2.2. Characterization methods of carbons

2.2.1. Physico-chemical analyses

Moisture content of carbons (MC) was determined by drying accordingly to ASTM D2867-17 norm (ASTMD-2867-17, 2017). The moisture content (%) was calculated according to **Eqn. 1**:

$$MC\ (\%) = \frac{m_1 - m_2}{m_1} \times 100 \qquad \textbf{Eqn.1}$$

Where m_1 : mass of carbon before drying at 105°C; and m_2 : mass of carbon after drying.

The content of volatile matters has been analyzed following the norms NF M03-004 and ISO 562 (Muema *et al.*, 2024), (Muema *et al.*, 2026), (Nzi, 2020). The volatile matters content (Vs) was calculated using **Eqn. 2**:

$$Vs = \frac{(m_2 - m_3)}{m_2 - m_1} \times 100 \qquad \textbf{Eqn. 2}$$

Where m_1: mass of the empty crucible with its lid (g);
m_2: mass of the crucible with its lid and the anhydrous sample (g);
m_3: mass of the crucible with its lid and the ash residue (g).

The ash content (ask) was analyzed following the norms NF M03-004 and ISO 562 (Nzi, 2020), (Muema *et al.*, 2026). The relation (**Eqn. 3**) was used to calculate the content of ash on drying matter:

$$Ask = \frac{(m_3 - m_1)}{m_2 - m_1} \times 100 \qquad \textbf{Eqn. 3}$$

The content of fixed carbon (FC) was determined following the norms NF M03-004 and ISO 562 (Nzi, 2020), (Muema *et al.*, 2026). The fixed carbon in drying matter was calculated using **Eqn.4**.

FC = 100 - (Vs + Ask) **Eqn.4**

The pH at the Zero Point Charge (pH_{ZPC}) corresponding to the isoelectric pH, was determined according to the method described, elsewhere (Sanou, 2017).

In addition, the iodine value (I_{I2}) indicating the microporous structure of materials was determined according to the experimental protocol described in AWWA standard B 600-78 (Mahler and Persson, 2013), (Sanou, 2017). The iodine value index (I_{I2}) was calculated using the **Eqn. 5**:

$$I_{I_2} = 25.4 \times \frac{(20 - Vn)}{m} \quad \textbf{Eqn. 5}$$

With m : mass of carbon (g), and Vn: volume of thiosulfate at equilibrium (mL).

Methylene blue index (I_{MB}) is considered an indicator of the mesoporous nature of a material (Thirunavukkarasu *et al*., 2001), (Sanou, 2017), (Kafando *et al*., 2025), (Latifi *et al*., 2025). It was analyzed using an Ultraviolet-visible (UV-vis) spectrometer at wavelength of 664 nm according to the protocol described by Benadjemia *et al.* (2011).

$$I_{BM} = (C_i - C_f) \times \frac{V}{m} \quad \textbf{Eqn. 6}$$

With C_i and C_f : initial and final concentrations of MB (mg/L), respectively;
V : volume of the solution (L), and m : mass of activated carbon (g).

The Langmuir surface area was determined using the MB adsorption method described by Kra Ouattara *et al.* (2015). It was noted S_L (m^2/g) corresponding to the internal surface area of macropores and mesopores onto the carbon:

$$S_L = Q_m \times N_A \times S \quad \textbf{Eqn.7}$$

With Q_m : maximal capacity of Langmuir's isotherm in MB adsorption (mg/g) ;
N_A : Avogadro number ($6.022.10^{23}$ mol^{-1}) ;
S: occupied surface of one methylene blue molecule (175.10^{-20} m^2).

2.2.2. Thermal and chemical analyses

The SDT Q600 thermobalance (TA Instrument) was used for thermogravimetric analysis of carbons. A Setsys Evolution 16 analyzer (Setaram) equipped with an electronic microbalance was used to measure mass losses of up to 400 mg with a precision of 0.4 µg. The Fourier Transform infrared (FT-IR) spectrum of the carbons were recorded between 400 and 4000 cm^{-1} with a 4 cm^{-1} resolution using KBr method with a spectrometer (PLATINUM-ATR), controlled by ORIGIN software to evaluate surface chemical functions. The activated carbons were analyzed by X-ray fluorescence (XRF) and XP CEN/TS 15104 norm in order to determine some chemical elements. A Si(Li) X-ray detector (Canberra) was used to determine the chemical composition of the activated carbons using the GE-PXRF 73GEO method.

2.3 Analysis methods of emerging pollutants

2.3.1 Analysis of methylene blue

To analyze the concentration of methylene blue (MB), UV-Vis molecular absorption spectrometry was used with a UV-Vis spectrophotometer (Hach, DR-3900) at 664 nm. A calibration line $A = f(C)$ was plotted with MB standard solutions ranging from 1 to 5 mg/L to determine the unknown solution concentration. Experimentally, these MB standard solutions were obtained by diluting a 30 mg/L MB stock solution which was prepared by dissolution of MB salt in distilled water.

2.3.2 Analysis of total cyanide

Cyanide solutions were from dilution of cyanide solution 1000 mg/L prepared from dissolution of NaCN salt in distilled water. The total cyanide content was determined according to ISO 6703-1 and EPA 335.4 standards methods. The sample was treated with H_2SO_4 in the presence of $MgCl_2$ to release HCN from its free and complex forms. The gaseous HCN was trapped in a 0.1 M NaOH solution and the trapped cyanide was titrated with chloramine-T in presence of a pyridine-barbiturate complex. A spectrophotometer was used to quantify the total cyanide concentration at 578 nm.

2.4. Batch adsorption experiments

Batch experiments were conducted using synthetic solutions of MB and cyanide, prepared from salts in the laboratory. The influence of operating parameters such as stirring speed, contact time, activated carbon mass, initial pH, and initial pollutant concentration was studied requiring their optimization. Each experiment was repeated three times and the average values of MB and cyanide concentrations were used for the calculations.

2.4.1 Removal of methylene blue

Both carbons namely CA1 and CA2 were used in MB removal experiments. To evaluate the effect of pH, different MB solutions with pH values ranged from 3 to 11 were prepared by adjustment with 1M H_2SO_4 and 1M NaOH solutions, under operating conditions such as 50 mL of MB solution 15 mg/L, 0.3 g of carbon during 60 min of contact at 150 rpm and room temperature (25°C). In addition, the rotation speed was varied from 50 to 220 rpm using 50 mL of a synthetic MB solutions of 15 mg/L, 0.3 g of carbon and 60 min of contact. For the contact time, it was varied from 5 to 100 min using 50 mL of a MB solutions of 15 mg/L and 0.30 g of carbon with stirring at 150 rpm. Moreover, the amount of activated carbon was varied from 2 g/L to 10 g/L by adding 0.1 to 0.5 g of activated carbon to 50 mL of MB solutions in each Erlenmeyer.

2.4.2 Removal of Cyanide

After the MB experiments carried out with both activated carbons, only CA2 was in quantity to be tested in cyanide removal experiments in order to compare its adsorption efficiency with the one of clays, widely used in our lab. The quantity of CA1 could not be possible to use in cyanide removal experiments.

To study the influence of pH, cyanide solutions (150 mL) with pH values between 9 and 14 were prepared by dissolving sodium cyanide in double-distilled water. The total cyanide content was analyzed after 24 hours of stand after the treatment under the operating conditions such as 1.5 g of carbon, 150 mL of cyanide solution 500 mg/L, 60 min of contact at 150 rpm and room temperature.

The influence of stirring was studied between 50 and 250 rpm using 150 mL of cyanide solutions and 10 g/L of carbon amount at 25°C. By varying the contact time from 10 to 180 min, 150 mL of cyanide solutions 500 mg/L and pH 11 were added to 1.5 g of CA2 at 150 rpm for a contact time.

Cyanide adsorption tests were performed by varying the amount of carbon between 2 and 15 g/L with cyanide solutions (pH > 11) of concentration 500 mg/L for 30 min of contact under stirring at 150 rpm. Each experiment was repeated three time in order to use the average value of pollutant concentration.

The removal percentage of pollutant (%R) was calculated according to the **Equation 8**:

$$\%R = \frac{C_0 - C_e}{C0} * 100 \qquad \textbf{Eqn.8}$$

With C_0 and Ce : initial and equilibrium concentrations of pollutant in the medium ($mg.L^{-1}$).

The adsorption capacity (Q_e) expressed in mg/g was calculated as wells:

$$Q_e = \frac{C_O - C_t}{m} x\ V \qquad \textbf{Eqn.9}$$

Where C_0 and C_t : initial and equilibrium concentrations of pollutant in the medium ($mg.L^{-1}$);
m : mass of carbon (g); and V : volume of the solution (L).

2.5 Modelling of experimental data

The experimental data obtained with varying contact time were applied to the pseudo-first-order and pseudo-second-order kinetic models described by Lagergren's equation and the one of Ho and Mckay (Sanou, 2017). The linearized form of the pseudo-first-order model is given by the **Eqn. 10**:

$$\ln (q_e - q_t) = \ln q_e - k_1 t \qquad \textbf{Eqn.10}$$

where q_e and q_t: adsorption capacity at equilibrium and the time t, respectively (mg/g); and k_1 : kinetic constant of pseudo-first order (min^{-1})
The equation of the plot of $\ln(q_e - q_t) = f(t)$ allows to determine the kinetic constants (K_1, qe and R^2).

The following equation (**Eqn. 11**) described the pseudo-second order model:

$$\frac{t}{qt} = \frac{1}{qe} t + \frac{1}{k2qe2} \qquad \textbf{Eqn.11}$$

where q_e and q_t: adsorption capacity at equilibrium and the time t, respectively (mg/g);
k_2 : kinetic constant of pseudo-second order (g. $mg^{-1}.min^{-1}$)
The kinetic constants (K_2, qe and R^2) were determined from the equation of the plot $\frac{t}{qt} = f(t)$.

Data obtained experimentally with the variation of initial concentration have been applied to Langmuir and Freundlich isotherm models.
The linear form of Langmuir isotherm is given by the **Eqn. 12** (Sanou, 2017):

$$\frac{C_e}{Q_e} = \frac{1}{K_L Q_m} + \frac{C_e}{Q_m} \qquad \textbf{Eqn.12}$$

With K_L : equilibrium constant of Langmuir (L/mg); and Q_m *and* Qe: maximal and equilibrium adsorption capacities, respectively (mg/g).
The values of K_L and Q_m were obtained from the graphic $C_e / Q_e = f(C_e)$.

The **equation 13** represents the linear form of Freundlich isotherm (Sanou, 2017), (Kaboré, 2025):

$$\ln Q_e = \ln K_f + n.\ \ln C_e \qquad \textbf{Eqn.13}$$

With K_f: constant of Freundlich linked to the adsorption capacity; C_e : concentration of pollutant in the solution (mg/L); and n : index of Freundlich measuring the adsorption intensity.
The values of K_f et n were obtained from the graphic representation $\ln Q_e = f(\ln C_e)$. The modelling of isotherms and kinetics was carried out in order to explain the mechanism of MB or cyanide adsorption onto the activated carbons.

3. Results and Discussion

3.1 3.1. Characteristics of activated carbons

3.1.1. Physicochemical properties

The immediate analyses of raw rice husks were focused on the moisture content (MC), the ask content (ask), the volatile matters (Vs) and the fixed carbon (FC) and the values of their parameters are

recorded in **Table 1**. The low moisture content (0.2% and 0.62%) suggests that the biomasses (LRH and RRH) are slightly hydrated. The ash content (22%) indicates that the raw rice husk (RRH) is mainly composed of silica. After leaching, this content decreases slightly to 15% due to the removal or dissolution of some mineral compounds during the leaching process (Borges *et al.*, 2016). The volatile matter content of 62% in the RRH indicates a significant proportion of volatile organic compounds. After leaching, this content was decreased to 46%, suggesting a reduction in soluble compounds.

The fixed carbon content in the RRH (16%) is relatively low, indicating rapid combustion with a low production of residual carbon. The increase of this rate to 39% in the LRH would be due to a loss of soluble matter during the leaching process (Chen *et al.*, 2012), (Sanou *et al.*, 2019).

Table 1. Physico-chemical properties of rice husks

Biomass	MC (%)	Ask (%)	Vs (%)	FC (%)
RRH	0.20	22	62	26
LRH	0.62	15	46	39

The characterization of activated carbons concerned some physico-chemical properties such the iodine index (I_{I2}), methylene blue index (I_{MB}), Langmuir's surface area (S_L) and moisture content (MC) and all values are summarized in **Table 2**. The value of iodine index of AC increased after leaching (from 567 to 635 mg/g), indicating an improvement in its porosity and adsorption capacity due to the removal of impurities (Mohan and Pittman, 2007). The low value of I_{MB} in carbons (4.95 mg/g) suggests a low adsorption capacity for organic compounds with the size of methylene blue. Furthermore, the higher iodine values compared to the methylene blue values suggested that the carbons may have a dominance of micropores with a high microporosity (Lekbir and Bekraoui, 2017). All the prepared carbons have an acid pH at zero-point charge (pH_{ZPC}) indicating the availability to adsorb a cationic pollutant such as methylene blue.

Table 2. Physico-chemical properties of activated carbons

Parameter	CA1	CA2
pH_{ZPC}	3.43	5.76
I_{BM} (mg/g)	4.95	4.94
I_{I2} (mg/g)	635	567
S_L (m^2/g)	135	134
MC (%)	2.3	1.7

3.1.2 Elemental chemical composition of carbons

X-ray fluorescence analysis and the application of XP CEN/TS 15104 norm yielded the chemical composition and the results are recorded in **Table 3**.

Table 3. Elemental chemical composition of carbons

Carbon	%C	%H	%O	%Si	%N	%S	Total
CA1	41.7	14.3	16.91	26.8	0.08	0.14	99.93
CA2	41.8	11.9	21.1	24.91	0.05	0.2	99.96

It was noticed that carbon and silicon were the predominant elements in the carbons. This predominance of carbon content in the AC confirms its carbonaceous structure, resulting from the

presence of cellulose, hemicellulose, and lignin in the rice husks. Leaching removed some of the mineral oxides and significantly reduced the apparent silicon content by removing amorphous silica.

3.1.3. Thermogravimetric properties

The **Figure 2** shows the DTG/TG thermogram of the raw biomass. The evolution of mass loss during the thermal treatment of raw rice husks indicates three stages of thermal degradation. The first stage ($T \leq 150°C$) with a mass loss of 10%, corresponds to the desorption of water from the pores of the rice husks along with the decomposition of hemicelluloses. The second stage ($150°C < T \leq 400°C$), with a mass loss of 45%, relates to the desorption of structural water from the cellulose and the breaking of the C-C and C-O chains. The final stage ($T > 400°C$), with a mass loss of 23%, is attributable to the degradation of lignin. These results confirm the lignocellulosic nature of rice husks for applications in combustion process under various conditions.

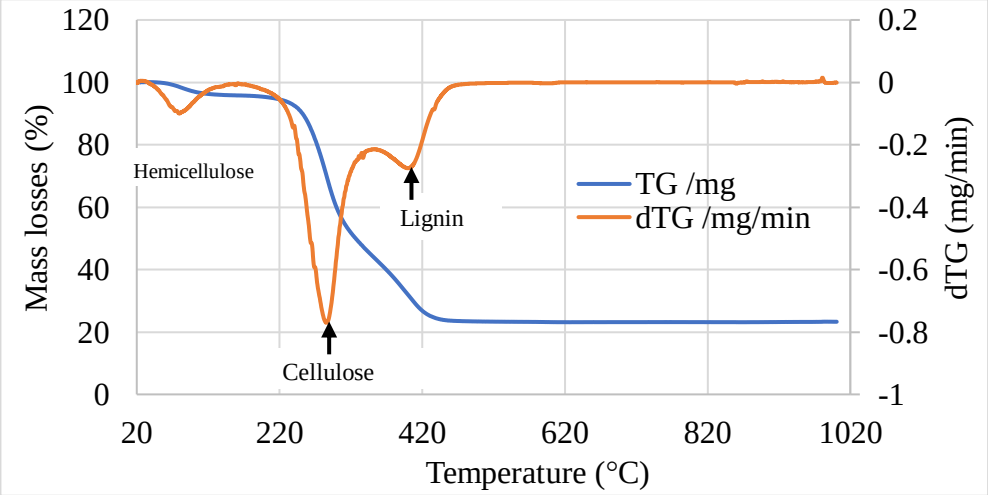

Figure 2. The dTG/TG spectrum of rice husks

3.1. 4. Chemical functions at the carbons surface

Figure 3 shows the infrared spectrum of activated carbons and the analysis of which allows to identify the vibration bands. The weak band between 3600 and 3200 cm^{-1} indicates the presence of hydroxyl (O-H) groups, due to residual moisture or phenolic compounds (Das, 2014).

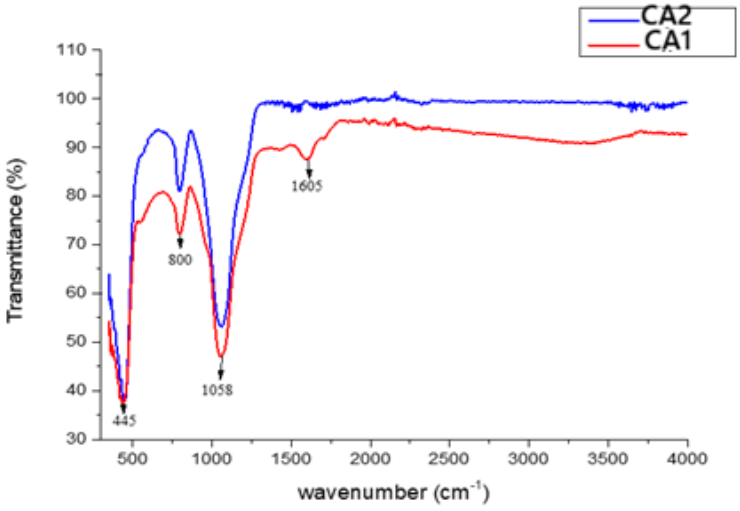

Figure 2. Infrared spectra of activated carbons

The band around 1605 cm^{-1} is characteristic of the C=C stretching vibrations of lignins. The high-intensity band centered at 1058 cm^{-1} is attributable to the C-O stretching vibration of phenolic compounds (Cellulose and hemicellulose) or polymers. Finally, the peak around 445 cm^{-1} is associated with the Si-O vibration, confirming a high mineral content (Leeruang, 2012). This spectrum suggests the presence of organic compounds such as cellulose, lignins, and hemicelluloses.

3.3 Depollution of wastewater contaminated by methylene blue and cyanide

3.2.1. Evaluation of the operating conditions on the adsorption of pollutants

3.2.1.1. Influence of initial pH

Experimental results on MB removal revealed two phases (**Figure 4a**). A rapid adsorption between pH 3 and 5 indicates a progressive removal of MB up to 97% due to the repulsion between the positive surface of carbons and MB form (Ahmad *et al.*, 2020), (Thuong Bui *et al.*, 2022). A constant phase between pH 5 and 11 indicates a high removal of MB due to the attraction force between the negative surface and cationic form of methylene blue (Ahmad *et al.*, 2020).

In this study, cyanide solutions were prepared at basic pH levels ranging from 9 to 14 (**Figure 4b**). Results presented in **Figure 4b** showed a biphasic curve. A progressive increase in the cyanide removal rate was observed between pH 9 and 11, due to the attraction between the positive surface and the anionic form of cyanide (CN^-). The constant phase between pH 11 and 14 indicates the stabilization of cyanide under strongly alkaline conditions.

These observations are in agreement with the mechanisms of cyanide degradation in solution, which indicates that a pH ≥ 11 inhibits HCN formation and prevents cyanide degradation (Kaboré *et al.*, 2024), (Sory *et al.*, 2024). For subsequent experimental tests, solutions were prepared at pH ≥ 11 to ensure the stability of cyanide in solution.

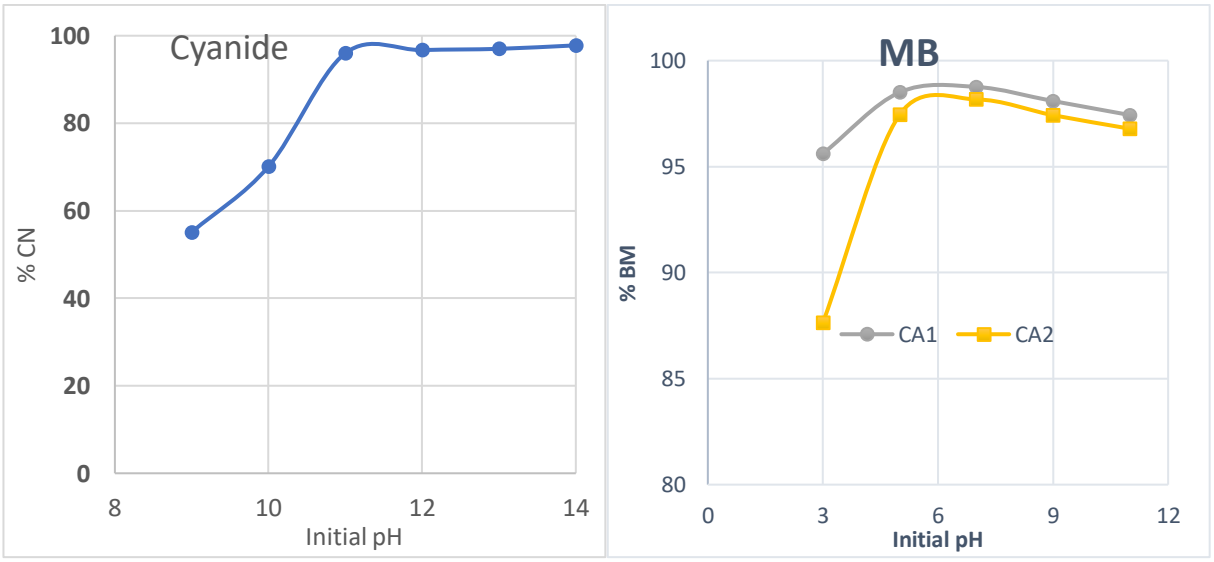

Figure 4. Influence of initial pH on MB and cyanide removal

3.2.1.2. Effect of stirring speed

The **Figure 5** indicates the variation of adsorption rate as function of the stirring speed. The pattern in **Figure 5a** showed an optimum at 150 rpm with a MB removal rate of 99% and 98% using CA1 and CA2, respectively. Above 150 rpm, the removal rate of MB remained constant. The obtained results are in agreement with the literature data which revealed the optimal stirring at 150 rpm (Sanou, 2017), (Sory *et al.*, 2024). The **figure 5b** revealed a non-linear relationship between stirring speed and

cyanide stability in two phases. From 50 to 150 rpm, the cyanide adsorption capacity increased with the stirring speed. Indeed, this stirring range promotes a uniform distribution of cyanide species, reducing local concentration gradients and limiting the cyanide degradation (Lee *et al.*, 2020), (Sory *et al.*, 2024). Above 150 rpm, a significant decrease in the total cyanide adsorption capacity is observed. This decrease could be explained by the forced desorption of cyanide fixed onto the pores of AC.

Experimental results indicated that 150 rpm is the optimal stirring speed. This value of 150 rpm was used for subsequent experiments.

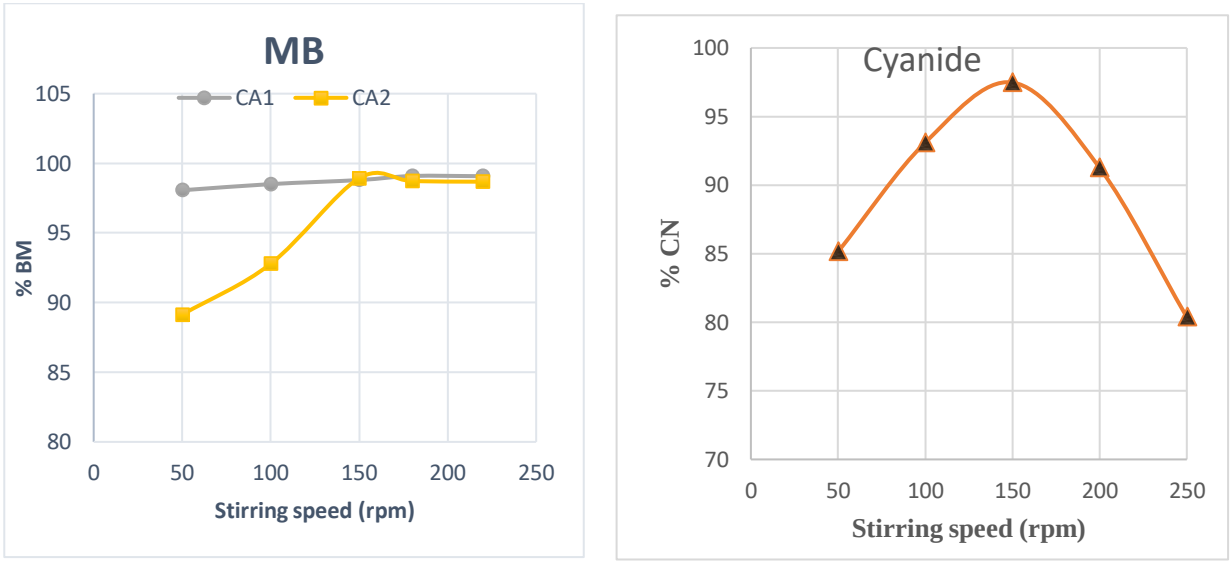

Figure 5. Effect of stirring speed on MB and cyanide removal

3.2.1.3. Effect of contact time

The variation of contact time (**Figure 6a**) revealed an increase in the MB removal rate over time occurring in two phases. A rapid phase between 0 and 40 min, indicates a quick bonding of methylene blue to the adsorption sites, with a removal rate varying from 87% to 98%. This could be attributed to the availability of sites, the number of which gradually decreases with the increasing time (Sanou, 2017). A second constant phase between 40 and 90 min, indicates a progressive saturation of the active sites onto the surface of carbons. After 40 min of treatment, the active sites are saturated, indicating of the achievement of equilibrium corresponding to treatment rates of 98% and 94%, respectively with CA1 and CA2. Consequently, the time of 40 min was kept for subsequent experiments on MB removal.

In the removal of cyanide, the **Figure 6b** shows a biphasic evolution of the treatment yield. Between 0 and 60 min, a quick adsorption of cyanide was observed, resulting from the combination of the high surface density of unoccupied active sites on the carbonaceous material and a significant concentration gradient at the interface of solution-adsorbent (Kaboré *et al.*, 2025). From 60 min to 180 min, the adsorption rate becomes constant, reflecting the progressive saturation of available active sites on the surface of carbons (Kaboré *et al.*, 2024). This stabilization suggests that a maximum adsorption capacity of carbons was reached. Thus, the equilibrium time was 60 minutes corresponding to 97.18% of effective depollution.

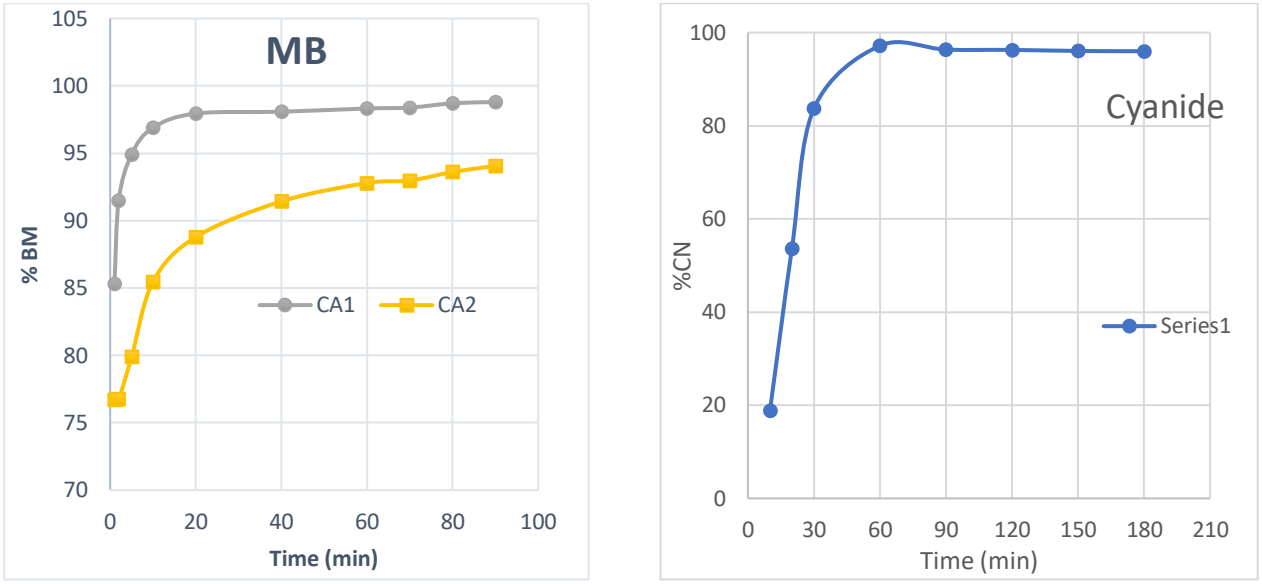

Figure 6. Effect of contact time on the removal of MB and cyanide

3.2.1.4. Effect of carbon amount

The effect of the activated carbon amount was studied between 2 and 10 g/L and results indicated an increase in the MB removal rate with increasing of carbon amount (**Figure 7a**). Analysis of this figure shows that the variation of the CA1 dose has no significant influence on MB removal, indicating early saturation of the adsorption sites. Using CA2, the removal rate increased from 86% to 97.48% with the carbon amount, indicating an optimum at 8 g/L where the efficiency of CA2 stabilized to be constant. Consequently, the value of 8 g/L will be considered the optimum amount for subsequent analyses.

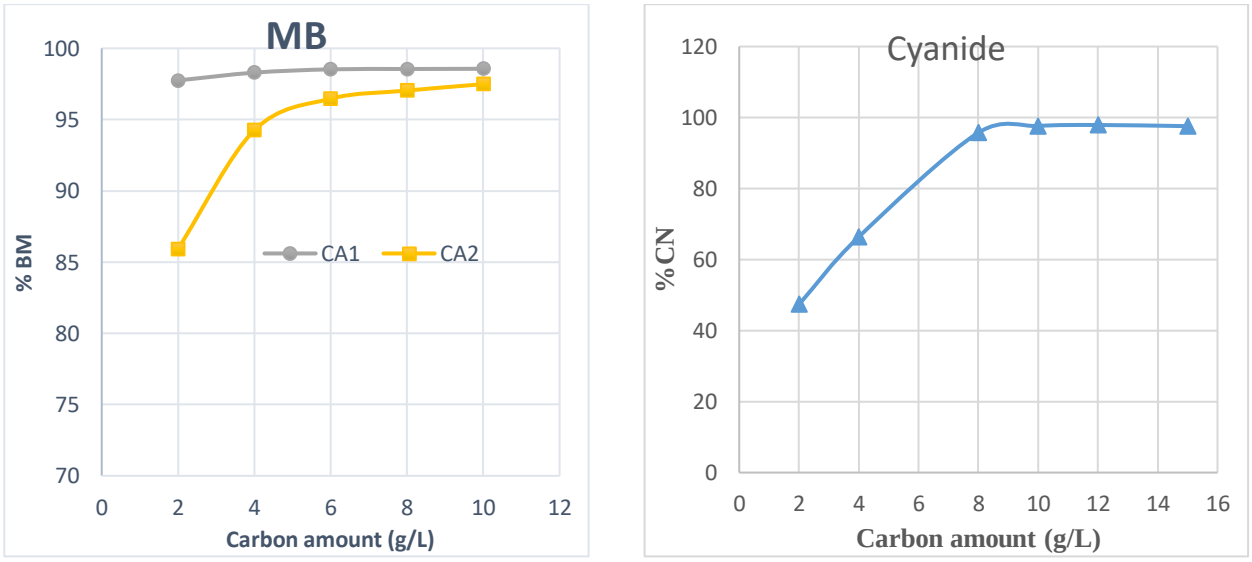

Figure 7. Effect of carbon amount on the removal of MB and cyanide

By removing the cyanide from wastewater using the carbon amount ranged from 2 to 15 g/L, the experimental results (**Figure 7b**) show a biphasic curve. For doses of 2 to 10 g/L, the insufficient quantity of carbon provides a limited specific surface area, rapidly saturating the available adsorption sites (Kaboré *et al.*, 2024). The adsorbent/adsorbate ratio is unbalanced, leading to incomplete coverage of cyanide ions. For doses beyond 10 g/L, the surface area becomes sufficient to adsorb almost of the

cyanide (>97%). Adsorption process achieved an equilibrium state from where the increase of the amount doesn't significantly improve the remediation efficiency (Kaboré *et al*., 2024). The amount of 10 g/L was optimal suggesting a complete surface coverage.

3.2.2. Study of the mechanism of MB and cyanide adsorption

3.2.2.1. Isotherm models

To determine the relationship describing the distribution of pollutant between the surface of the carbons and the water, the experimental data from the variation of initial concentration of pollutant were applied to Langmuir and Freundlich isotherm models. The graphical representations of which are given in **Figures 8** and **9**, respectively for the removal of MB and cyanide in solution. The constants of these isotherm models are listed in **Table 4**.

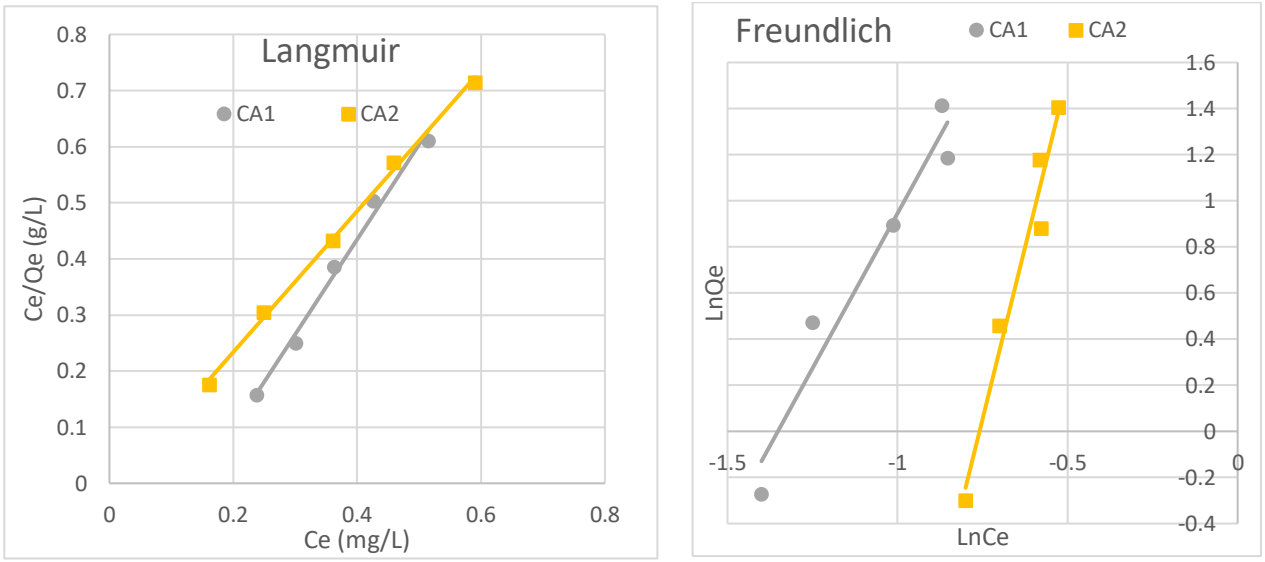

Figure 8. Representation of Langmuir and Freundlich isotherms in MB removal

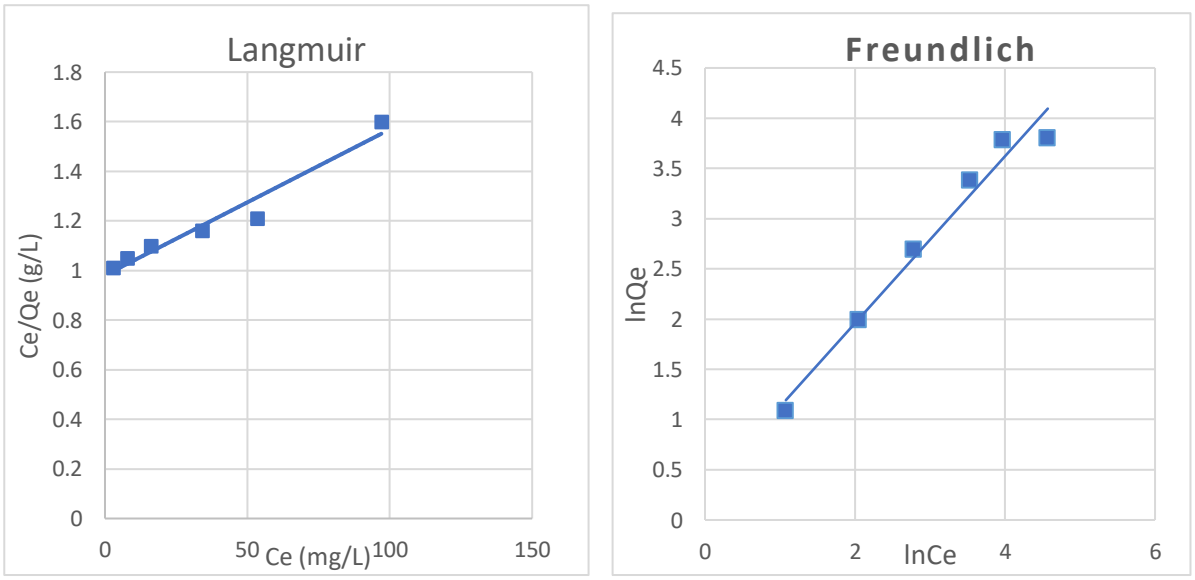

Figure 9. Representation of Langmuir and Freundlich isotherms in cyanide removal

Table 4. Constants of Langmuir and Freundlich isotherms

Carbon	Langmuir isotherm				Freundlich isotherm			Q_{exp} (mg/g)
	Q_m (mg/g)	$\|K_L\|$ (L/mg)	R^2	ΔG (kJ/mol)	K_F (mg/g)	n	R^2	
CA1-MB	2.79	7.30	0.99	-2.11	7.84	3	0.94	2.76
CA2-MB	2.59	7.14	0.99	-2.14	9.58	6	0.96	2.74
CA2-CN	169.49	0.06	0.96	-1.73	134.4	1	0.87	170

Data analysis (**Table 4**) shows that the correlation coefficients (R^2 = 0.99) are higher and close to unity (1) with the Langmuir isotherm. In addition, the values of theoretical maximum capacity (Q_m) obtained with this model are similar to the experimental values (Q_{exp}). These results conclude that the removal of MB and cyanide was correlated with the Langmuir isotherm, indicating a monolayer process (Kaboré, 2025). The separation factor (R_L) indicating if the process is favorable or not, was calculated using the relationship given by the **Eqn. 13** (Sanou, 2017), (Jency and Krishnaveni, 2021):

$$R_L = \frac{1}{(1+K_L.C_0)} \qquad \textbf{Eqn. 13}$$

Calculations showed that the values of R_L were ranged from 0.005 to 0.027, indicating a process favorable to the adsorption because $0 < R_L < 1$ (Sanou, 2017). The negative values of the free energy calculated by the relation $\Delta G = -RT\ LogK_L$ (**Table 4**) indicate that the removal of MB and cyanide onto the carbons has been occurred by a spontaneous process. Consequently, the removal of MB and cyanide occurs by a monolayer adsorption onto localized sites through an irreversible process.

3.2.2.2. Kinetic models

The graphs $ln\ (qe - qt) = f(t)$ of the pseudo-first-order kinetic model allow the speed constant to be determined from the slope of the lines (**Figures 10a** and **11a**). The graphs $t/qt = f(t)$ of the pseudo-second-order model are given in **Figures 10b** and **11b**. The values of the constants for these kinetic models are listed in **Table 5**.

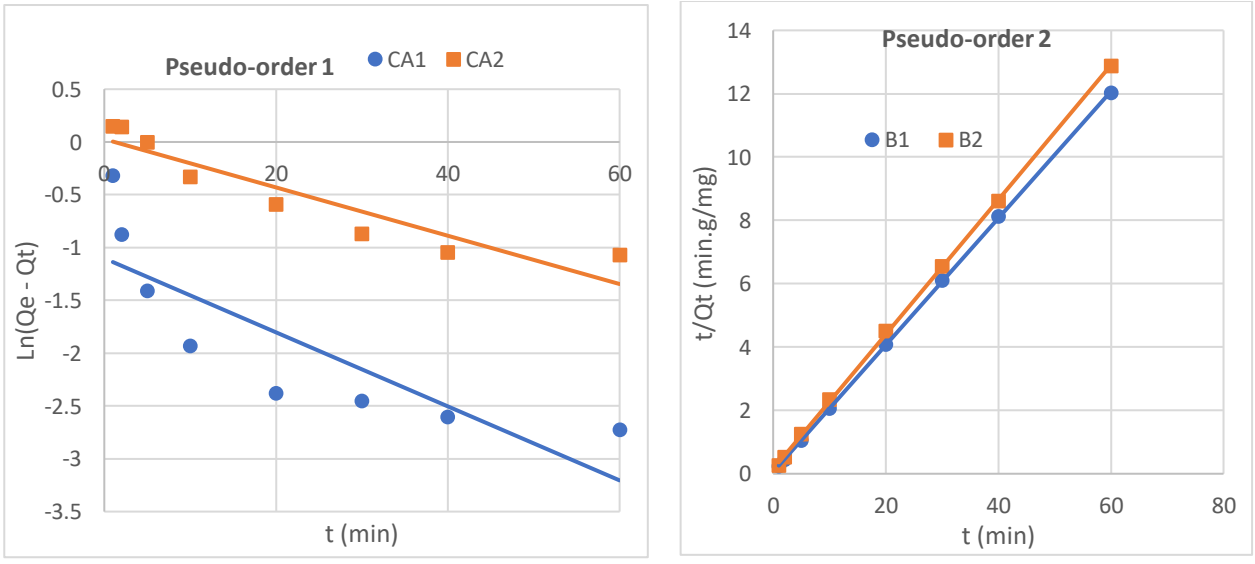

Figure 10. Representation of kinetic models in MB removal

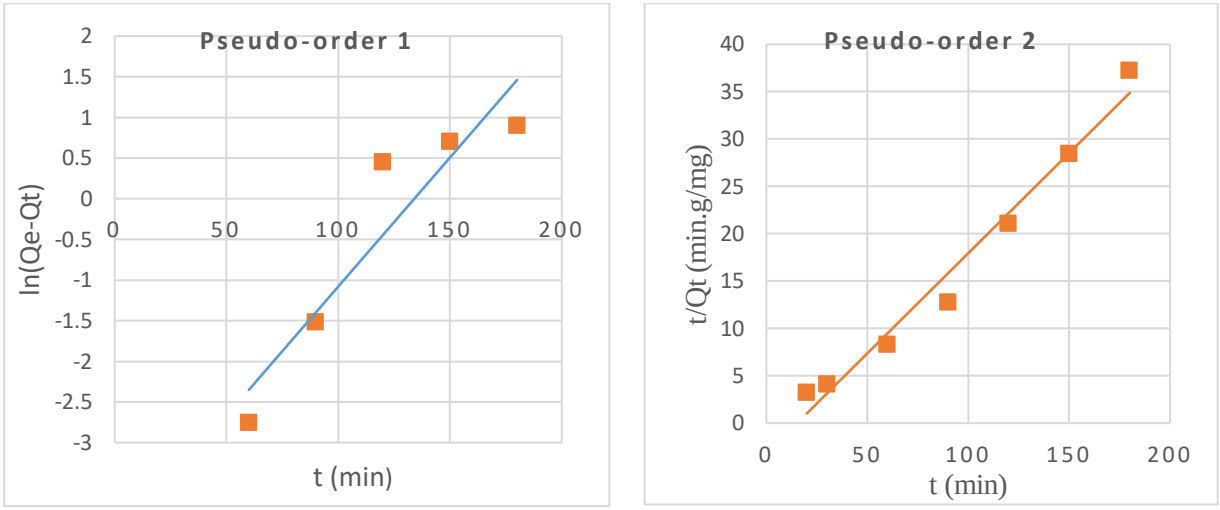

Figure 11. Representation of kinetic models in cyanide removal

Table 5. Constants of kinetic models in the removal of MB and cyanide

Carbon	Pseudo-order 1			Pseudo-order 2			
	K_1 (min^{-1})	Q_m (mg/g)	R^2	K_2 (g/min.mg)	Q_m (mg/g)	R^2	Q_{exp} (mg/g)
CA1-MB	0.04	0.33	0.70	0.71	2.49	0.99	2.5
CA2-MB	0.02	1.02	0.87	0.31	2.70	0.99	2.5
CA2-CN	0.03	10.01	0.88	0.01	47.25	0.97	48.59

Data in **Table 5** showed that with the pseudo-second-order model, the correlation coefficients (R^2 = 0.99) are higher and close to unity (1). Furthermore, the theoretical adsorption capacities (Q_m) are close to the experimental values (Q_{exp}). Therefore, the removal of MB and cyanide has been occurred following a pseudo-second-order kinetic suggesting a chemisorption process (Sanou, 2017), (Jency and Krishnaveni, 2021), (Kaboré, 2025). However, the investigation on the real mechanism of adsorption can be explored using other mathematical model, desorption tests and analysis by FT-IR spectrum of exhausted carbons.

Conclusion

This study evaluated the potential of activated carbons as an adsorbent for the removal of cyanide and MB from wastewater, combining experimental and theoretical approaches. Activated carbons produced from rice husks exhibited microporous structures with functional groups favorable to the adsorption of cyanide and MB. Elemental analysis of carbons showed the predominant presence of carbon, silicon, hydrogen, and oxygen. The decontamination process was strongly influenced by operating parameters such as stirring speed, contact time, carbon amount, and the initial pH of the medium. Cyanide removal reached a rate of 97% under optimal conditions (pH >11, 150 rpm, 10 g/L, 60 min). While the BM removal reached 98% for 40 min of contact. The removal of cyanide and MB was best described by the Langmuir isotherm, indicating a monolayer process with pseudo-second-order kinetics. In addition, the process was probably controlled by chemical interactions. This study carried out with synthetic solutions, will be applied using a natural wastewater and an additional characterization of carbons using SEM/EDX, BET/BJH and XRD analyses will be realized.

Acknowledgement: The international institute of water and environment Engineering, and Polytechnical School of Ouagadougou are acknowledged for their technical support, enable to carry out this study.

Disclosure statement: *Conflict of Interest:* The authors declare that there are no conflicts of interest.
Compliance with Ethical Standards: This article does not contain any studies involving human or animal subjects.

References

Ahmad A., Khan N., Giri B. S., Chowdhary P., Chaturvedi P. (2020) Removal of methylene blue dye using rice husk, cow dung and sludge biochar: Characterization, application, and kinetic studies. *Bioresource technology*.306, p. 123202.

Akartasse N., Azzaoui K., Mejdoubi E., Hammouti B., Elansari L.L., Abou-salama M., Aaddouz M., Sabbahi R., Rhazi L., Siaj M. (2022), Environmental-Friendly Adsorbent Composite Based on Hydroxyapatite/ Hydroxypropyl Methyl-Cellulose for Removal of Cationic Dyes from an Aqueous Solution, *Polymers*, 14(11), 2147; https://doi.org/10.3390/polym14112147

American Society for Testing and Materials (2017). ASTM D2867-17, Standard Test Methods for Moisture in Activated Carbon, describes a gravimetric method for determining moisture content by measuring mass loss upon drying, pp.13-14

Benadjemia M., Milliere L., Reinert L., Benderdouche N., Duclaux L. (2011) Preparation, characterization and Methylene Blue adsorption of phosphoric acid activated carbons from globe artichoke leaves. *Fuel Processing Technology* 92(6):1203-1212. DOI:10.1016/j.fuproc.2011.01.014

Bhatnagar A., Sillanpää M. (2011). Utilization of agro-industrial and municipal waste materials as potential adsorbents for water treatment: A review. *Chem. Eng. J.* 168(1), 493-507.

Borges P. H. R., Nunes V. A., Panzera T. H., Schileo G., Feteira A. (2016) The influence of rice husk ash addition on the properties of metakaolin-based geopolymers. *The Open Construction and Building Technology Journal*.10(Suppl 3: M4), 406-417. DOI: 10.2174/1874836801610010406.

Botz M. (2001) Overview of cyanide treatment methods. *Mining Environmental Management*. 28-30.

Chen M. (2012) Faisabilité technique et environnementale de l'utilisation dans des matériaux de construction cimentaires de cendres d'incinération de boues de station d'épuration. Thèse de doctorat, INSA /Lyon, France. 10.70675/9f43ebcaz4e90z48ebz8813z5a5d97bd491d

Chen Y., Wang X., Zhang S., Chen H. (2012) Biomass-based pyrolytic polygeneration system on cotton stalk pyrolysis: influence of temperature. *Bioressource Technology*. 107, 411- 418. http://dx.doi.org/10.1016/j.biortech.2011.10.074.

Das S. (2014) Characterization of activated carbon of coconut shell, rice husk and Karanja oil cake », PhD Thesis, National Institute of Technology Rourkela, India.

Dash R., Balomajumder C., Kumar A. (2009) Removal of cyanide from water and wastewater using granular activated carbon. *Chem. Eng*. J. 146(3), 408-413, https://doi.org/10.1016/j.cej.2008.06.021

Gao D., Li Z., Wen Z., Ren N. (2016). Occurrence and fate of phthalate esters in full-scale domestic wastewater treatment plants and their impact on receiving waters along the Songhua River in China. *Sci. Total Environ*. 565, 1034–1042. https://doi.org/10.1016/j.scitotenv.2016.06.094

Haoufazane, C., Zaaboul, F., Monfalouti, H.E., Jodeh S., Azzaoui K., Hammouti B., Tihmmou R., Salghi R. & Kartah B.E. (2025). Enhanced removal of C.I. direct black 80 by phosphoric acid activated plant biomass supported by DFT insights. *Sci Rep* 15, 40134 https://doi.org/10.1038/s41598-025-23886-z

Halet F., Yeddou A. R., Chergui A., Chergui S., Nadjemi B., Ould-Dris A. (2015) Removal of Cyanide from Aqueous Solutions by Adsorption on Activated Carbon Prepared from Lignocellulosic By-products. *J. Dispers. Sci. Technol*. 36 (12), 1736-1741, https://doi.org/10.1080/01932691.2015.1005311

Haruna A, Abdulkadir I, Idris SO. (2020). Photocatalytic activity and doping effects of $BiFeO_3$ nanoparticles in model organic dyes. *Heliyon*, 6, e03237. https://doi.org/10.1016/j.heliyon.2020.e03237

Hou D., Li D., Yang P., Li Y., Huang Q., Zhang G. (2020) Decomposition of cyanide from gold leaching tailings by using sodium metabisulphite and hydrogen peroxide. *Advances Mater. Sci. Eng.* p. 5 doi: 10.1155/2020/5640963

Jency M., Krishnaveni J. (2021) Adsorptive removal of dyes onto cost effective biomaterials a review. *J. Environ. Treat. Tech*. 9, n° 1, p. 218-223.

Kaboré R., Sanou Y., Konaté A., Paré S. (2024) Study of the Efficiency of Two Clays Soils for Cyanide Removal in Water: Kinetic and Equilibrium Modelling. *Asian J. Phys. Chem. Sci.* 12 (2), 1-14. https://doi.org/10.9734/ajopacs/2024/v12i2220.

Kaboré R. (2025) Matières premières argileuses : préparation, caractérisation et applications à l'élimination du cyanure des eaux. Thèse de doctorat unique, Université Joseph KI-ZERBO, Burkina Faso.

Kaboré R., Sanou Y., Tiendrebéogo R., Compaoré A., Konaté A., Paré S. (2025) Preparation and characterization of clay soils for applications in cyanide removal from mining wastewater. *J. Min. Mater. Character. Eng.* 13(1), 1-17. https://doi.org/10.4236/jmmce.2025.131001.

Kafando G. I., Kone M., Kaboré B., Kindo A., Karanga Y., Iname A., Yamma R., Sawadogo B.J., Tamboura S., Kutangila S. M., Bougouma M. (2025) Valorization of Corn Cobs into Activated Carbon through Chemical Activation and Evaluation of Their Methylene Blue Adsorption Performance for Contaminated Water Treatment. I*nter. Res. J. Pure and Appl. Chem.* 26(6), 138-159, 2025. DOI: 10.9734/irjpac/2025/v26i6965.

Kra Ouattara D., Kouadio N.A., Atheba G. P., Coulibaly B., Allou N. B., Gbassi K. G., Trokourey A. (2015) Modélisation des propriétés adsorbantes de charbons activés issus de deux variétés d'Acacia (Auriculiformis and Mangium). *Inter.l J. Innovation Scientific Research*. 13, n° 2, 542-553.

Kumar P., Gupta K., Singh K. (2016) A comprehensive review on the production and applications of activated carbon from agricultural residues. *Renewable and Sustainable Energy Reviews*. 55, 1095-1110.

Latifi S., Saoiabi S., Alanazi M. M., Boukra O., Krime A., El Hammari L., Azzaoui K., Hammouti B., Hanbali G., Jodeh S., Saoiabi A., Sabbahi R., Algarra M., Abidi N. (2025), Low-Cost Titania-Hydroxyapatite (TiHAp) nanocomposites were synthesized for removal of Methylene blue under Solar and UV irradiation, *Next Materials*, 8, 100859, ISSN 2949-8228, https://doi.org/10.1016/j.nxmate.2025.100859

Lee S., Kim J. H., Park C. W., Yoon J. Y. (2020). Mixing effects on cyanide stability in alkaline solutions. *J. Hazardous Mater.* 398(5), 122948.

Leeruang U. (2012) Purification of biodiesel by adsorption with activated low silica bentonite. Master Thesis, Chulalongkorn University, Thailand.

Lekbir K., Bekraoui A. (2017) Etude de la dépollution des eaux usées par des adsorbants organométallique (TMA-Ni) » Thèse de doctorat, Université Ahmed Draia-ADRAR, Algérie.

Mähler J., Persson I. (2013) Rapid adsorption of arsenic from aqueous solution by ferrihydrite-coated sand and granular ferric hydroxide. *Applied Geochemistry*. 37, 179-189.

Mohan D., Pittman Jr C. U. (2007) Arsenic removal from water/wastewater using adsorbents—a critical review. *J. Hazardous Mater*. 142, n° 1-2, 1-53.

Mohan D., Singh K.P., Singh V. K. (2014) Removal of cyanide from aqueous solutions using activated carbon: A review. *Environ. Sci. Pollution Research*. 21(1), 1-15.

Moussavi G., Khosravi R. (2011). The removal of cationic dyes from aqueous solutions by adsorption onto pistachio hull waste. *J. Hazard. Mater*. 185,302-308. doi:10.1016/j.jhazmat.2010.09.036

Muema F. M., Richardson Y., Keita A., Sawadogo M. (2024) An interdisciplinary overview on biochar production engineering and its agronomic applications. *Biomass and Bioenergy*. 190, p. 107416. https://doi.org/10.1016/j.biombioe.2024.107416

Muema F. M., Sawadogo M., Keita A., Richardson Y., Sawadogo F., Sanou Y. (2026) Integrating Biochar to Sustain Lettuce Production in Sandy Soils of Burkina Faso Under Water-Limited Conditions. *Sustainability*. 18, 4592. https://doi.org/10.3390/su18094592

Nzi Hou A. (2020) Handbook on characterization of biomass.p.ZT DOI : https://doi.org/10.1007/978-3-030-35020-8D.

Sakr F., Sennaoui A., Elouardi M., Tamimi M., Assabbane A. (2015) Adsorption study of Methylene Blue on biomaterial using cactus. *J. Mater. Environ. Sci*. 6, nº 2, 397-406.

Sanou Y. (2017) Etude des performances des charbons actifs, du granulé d'hydroxyde ferrique et la latérite pour l'élimination de la demande chimique en oxygène, du calcium et de l'arsenic des eaux », Université Ouaga I Pr Joseph KI-ZERBO, Burkina Faso.

Sanou Y., Pare S., Baba G., Segbeaya N. K., Bonzi-Coulibaly L. Y. (2016) Removal of COD in wastewaters by activated charcoal from rice husk. *J. Water Sci.* 29(3), 265-277.

Sanou Y., Nguyen T. T. P., Pare S., Nguyen V. P. (2019) The removal As (V) from aqueous solutions using Ferromagnetic Activated Carbon: equilibrium and kinetic studies. *Rev. Sci. Eau.*32(2), 179-192. DOI: 10.7202/1065206ar.

Sory D., Sanou Y., Kaboré R., Paré S. (2024) Efficiency of Two Laterites in Cyanide Removal from Aqueous Solutions: Equilibrium and Kinetic Studies. *Sci. J. Anal. Chem.* 12 (3), 38-45. https://doi.org/10.11648/j.sjac.20241203.12.

Tchuifon D.R.T., Anagho S.G., Ketcha J.M. (2016) Adsorption des phénols via des charbons de balles de riz. Thèse de doctorat unique, Université de Dschang, Cameroun, pp. 60-90.

Tchounwou P., Yedjou B., Patlolla C. G., Sutton A. K., D. J. (2012) Heavy Metal Toxicity and the Environment. *Experientia Supplementum* 101, 133-164. https://doi.org/10.1007/978-3-7643-8340-4_6

Thirunavukkarasu O. S., Viraraghavan T., Subramanian K. S. (2001) Removal of arsenic in drinking water by iron oxide-coated sand and ferrihydrite—batch studies. *Water Quality Research Journal*. 36, nº 1, 55-70.

Thuong Bui H. *et al.* (2022) Removal of methylene blue from aqueous solution by biochar derived from rice husk. *Vietnam J. Earth Sci.* 44(2), 273-285. https://doi.org/10.15625/2615-9783/16998